Phase Equilibria of Alkanes in Natural Gas Systems. 1. Alkanes in Methane

David Suleiman and Charles A. Eckert*

School of Chemical Engineering and Center for Specialty Separations, Georgia Institute of Technology, Atlanta, Georgia 30332-0100

We report the application of a new chromatographic technique to measure capacity factors for several *n*-alkanes (C_7H_{16} to $C_{36}H_{74}$) in methane in the range 293.2–423.2 K, and at 120–240 bar. Regular solution theory is used to characterize the stationary phase to permit the calculation of infinite dilution activity coefficients, γ_i^∞; this allows the conversion of the capacity factors to estimates of the solubility of the *n*-alkanes in methane. The solubility results are in good agreement with those data available from more conventional techniques. However, the new method permits investigations of much lower values of the solubility, especially for heavier hydrocarbon solutes, typically inaccessible with other methods. The capacity factor data can also be differentiated to yield directly partial molar volumes and partial molar enthalpies at infinite dilution. The phase equilibrium information obtained with this method provides valuable data for understanding size differences, as well as for helping to ameliorate solid deposition problems of natural gas companies.

Introduction

Information on the phase equilibria of *n*-paraffins in natural gas systems is important for both practical and theoretical purposes. First, such data are crucial in the design of natural gas pipeline systems, to avoid blockages caused by solidification of waxes, especially at low temperatures. However, such data also offer a unique opportunity to view systems with dispersion forces only, differing only by large differences in molecular size and shape. Such results are intermediate and complementary to the data of limiting activity coefficients for liquids, γ_i^∞, C_5H_{12} to $C_{16}H_{34}$, measured by headspace chromatography (Park, 1988; Cheong, 1989; Abraham *et al.*, 1990; Eikens, 1993), and the many data available for polymer systems. We hope these can contribute to a new understanding of size and shape effects.

Although numerous publications have investigated the phase equilibrium behavior of the lower *n*-alkanes (*e.g.*, C_2H_6, C_3H_8, and C_4H_{10}) in CH_4 (*e.g.*, Sage *et al.*, 1934, 1939, 1940a; Olds *et al.*, 1942; Reamer *et al.*, 1947, 1950; Magee *et al.*, 1982; Arai and Kobayashi, 1980; Henry *et al.*, 1977; Arai *et al.*, 1974; Chen *et al.*, 1973), there are very few phase equilibrium data for the liquid *n*-alkanes (*e.g.*, C_5H_{12} to $C_{16}H_{34}$) in CH_4 (*e.g.*, Sage *et al.*, 1940b, 1942; D'Avila *et al.*, 1976; Kaul and Prausnitz, 1978; Rijkers *et al.*, 1992a,b, 1993), and no data for the solid *n*-alkanes (*e.g.*, $C_{24}H_{50}$ to $C_{36}H_{74}$) in CH_4. Some of the liquid *n*-alkane solubility data in CH_4 (*e.g.*, Sage *et al.*, 1940b, 1942; D'Avila *et al.*, 1976; Kaul and Prausnitz, 1978), are only available at high temperatures (*e.g.*, 423–500 K), due to the low solubilities in CH_4.

Conventional methods for investigating solid solubilities in gases or supercritical fluids (SCFs) are hindered by various experimental limitations. The most common classical method would be a transpiration technique (Johnston and Eckert, 1981; Johnston *et al.*, 1982), where a flowing stream of compressed fluid is flowed over and equilibrated with a thermostated bed of pure solid and then depressurized and the solute collected and weighed. As the solute gets heavier, the time required becomes very large, and the amounts weighed become very small.

An attractive experimental alternative to the conventional methods is the chromatographic technique, which has been used extensively by several researchers to determine solubilities (Yonker *et al.*, 1987; Smith *et al.*, 1987; Barker *et al.*, 1988; Bartle *et al.*, 1990a,b), enhancement factors (Brown *et al.*, 1987), partial molar volumes and enthalpies at infinite dilution (van Wasen *et al.*, 1980; Shim and Johnston, 1991), and even cosolvent effects (Ekart et al., 1992, 1993). This method has many advantages: rapidity, small sample size, low purity requirements (since the impurities are separated in the chromatographic column), and the capability to provide phase equilibrium data at high temperatures or at low pressures where other techniques fail since the solubility is small, or simply because the solute may not be in its solid state.

However, this chromatographic method has not been applied to aliphatic substances in natural gas systems, primarily because of the limitations of the commonly-employed detectors. The *n*-alkanes are not UV-active, the flammable nature of the solvents (*e.g.*, methane/ethane) precludes the use of FID, and thermal conductivity is insensitive and inapplicable at elevated pressures. One might in principle use FTIR, or mass spectroscopy; however, a less expensive and easier alternative is the evaporative light scattering detector (ELSD), commonly employed in liquid chromatography. This light scattering detector modified for SCFs/dense gases proved to be highly efficient and reproducible for these saturated hydrocarbons.

This paper describes a chromatographic technique for the rapid and accurate determination of the solubilities of the *n*-alkanes in SCFs/dense gases. In addition, a database of experimental capacity factors and their corresponding solubilities is presented for the binary systems: *n*-alkanes from C_7H_{16} to $C_{36}H_{74}$ in CH_4, from 293.2 to 423.2 K and from 120 to 240 bar. Partial molar volumes and partial molar enthalpies at infinite dilution can also be calculated from the density and temperature derivatives of the

0021-9568/95/1740-0002$09.00/0

capacity factors, and some of these results are also presented.

Theory

In chromatography, the degree of retention of a solute depends upon its distribution between the mobile and stationary phases; it is characterized by a dimensionless capacity factor, k_i:

$$k_i = \frac{(t_i - t_o)}{t_o} \tag{1}$$

where t_i is the retention time of solute i, and t_o is the retention time of a solute that is not retained in the stationary phase. If one assumes equilibrium, k_i can also be represented as follows:

$$k_i = \frac{x_i}{y_i}\frac{V^s}{V^s_m}\frac{V^m_m}{V^m} \tag{2}$$

where x_i and y_i are the mole fractions of component i in the stationary and mobile phases, respectively. The molar volumes of the stationary and mobile phases in the chromatographic column are represented as V^s_m and V^m_m, while V^s and V^m are the physical volumes of the stationary and mobile phases, respectively. Phase equilibrium considerations then yield Φ_i^∞, the fugacity coefficient of solute i in the mobile phase at infinite dilution in terms of pressure, P, and Henry's constant of solute i in the stationary phase, $k_{H,i}$. If one assumes that the partial molar volume of solute i *in the stationary phase*, $\bar{V}_i$, is equal to its liquid molar volume, V_i, and introducing the pressure dependence on $k_{H,i}$, Φ_i^∞ becomes

$$\Phi_i^\infty = \frac{k_i k^\circ_{H,i}}{PV^m_m}\exp\left(\frac{V_i(P - P^\circ)}{RT}\right)\left|\frac{V^m V^s_m}{V^s}\right| \tag{3}$$

$k^\circ_{H,i}$ is Henry's constant between solute i and the packing material at the reference pressure P°. The ratio between vertical bars, $|V^m V^s_m/V^s|$, depends only on the chromatographic column, and should not vary significantly with pressure. One application of this derivation is obtaining solubilities for dilute systems (Yonker *et al.*, 1987; Smith *et al.*, 1987; Barker *et al.*, 1988; Bartle *et al.*, 1990a,b). In this approach, the conventional solubility expression for SCFs (Prausnitz *et al.*, 1986) is combined with eq 3 to provide the solubility of a solute i, from the chromatographic capacity factors, k_i

$$y_i = \left|\frac{P_{i,sat}V^s}{k^\circ_{H,i}V^m V^s_m}\exp\left(\frac{V_i(P^\circ - P_{i,sat})}{RT}\right)\right|\frac{V^m_m}{k_i} = |C_i(T)|\frac{V^m_m}{k_i} \tag{4}$$

where $P_{i,sat}$ is the saturation pressure (vapor or sublimation pressure depending on the physical state of the solute at the conditions studied). The left expression between vertical bars was called $C_i(T)$ by other researchers (Barker *et al.*, 1988; Bartle *et al.*, 1990a,b; Ekart *et al.*, 1992, 1993). In a given column, and for a given solute, $C_i(T)$ is a function of temperature only. In order to determine $C_i(T)$ for a particular solute and a particular temperature, one must measure at least one solubility data point at that temperature with an independent technique, or calculate it. Once $C_i(T)$ is known, the entire solubility isotherm can be determined rapidly from the chromatographic capacity factors.

Due to the lack of solubility data for the n-alkanes in CH_4, $C_i(T)$ was calculated as follows. For liquids with low

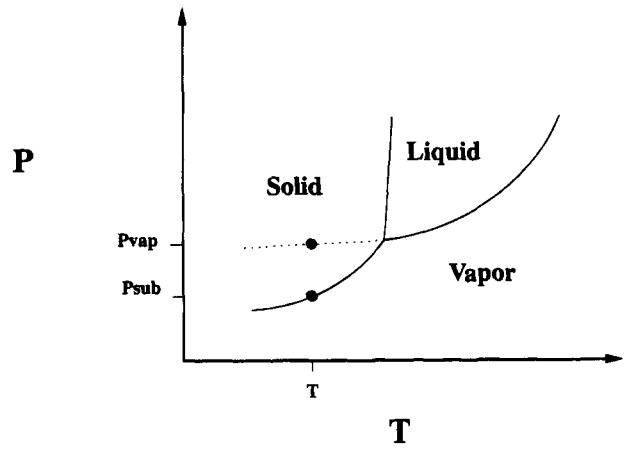

Figure 1. Pressure–temperature diagram for a pure substance.

$P_{i,vap}$, $C_i(T)$ reduces to

$$C_i(T) = \left|\frac{V^s}{V^m V^s_m}\right|\frac{1}{\gamma_i^\infty} \tag{5}$$

The expression between vertical bars, $|V^s/V^m V^s_m|$, can be obtained from the physical information provided by the manufacturer of the chromatographic column. γ_i^∞ is the activity coefficient at infinite dilution between the solute i and the stationary phase. In these nonpolar systems, γ_i^∞ may be obtained by an application of regular solution theory (RST) (Hildebrand *et al.*, 1970). Since the stationary phase is an octadecyl bonded phase to a silica support, and no solubility parameter for this material was available, a single experimental solubility datum for $C_{10}H_{22}$ in CH_4 at 313.2 K (Rijkers *et al.*, 1992a) was used to regress the constant $C_i(T)$, which provided γ_i^∞, and therefore the solubility parameter of the stationary phase. The solubility parameters for the n-alkanes and their temperature dependence were calculated using Fedors' group contribution method (Fedors, 1974). The isobaric thermal expansion coefficients of the n-alkanes, required to account for the temperature dependence of the solubility parameters, were obtained from Nikolic (1993).

For solids, the calculation of $C_i(T)$ requires an additional ratio, $P_{i,sub}/P_{i,vap}$, where $P_{i,sub}$ is the sublimation pressure and $P_{i,vap}$ is the vapor pressure of the hypothetical liquid (Figure 1):

$$C_i(T) = \left|\frac{V^s}{V^m V^s_m}\right|\frac{1}{\gamma_i^\infty}\frac{P_{i,sub}}{P_{i,vap}} \tag{6}$$

An important comment about this approach to obtain solubilities is that the derivation assumes that the fugacity coefficient does not change with concentration from the infinite dilution value. This assumption is only valid for very small solubilities (*e.g.*, $<10^{-2}$ mole fraction); for more soluble systems the concentration dependence of the fugacity coefficient should be considered.

Instrumentation and Equipment

The experiment described elsewhere (Suleiman *et al.*, 1993) has been modified for use with CH_4 (Figure 2). A gas booster (HASKEL AG-152) fills a high-pressure vessel with CH_4 at a target pressure, which feeds the pulse-free high-pressure syringe pump (ISCO 500D). To assure thermal equilibrium, the fluid/dense gas then goes through 2 m of stainless steel tubing immersed in a constant

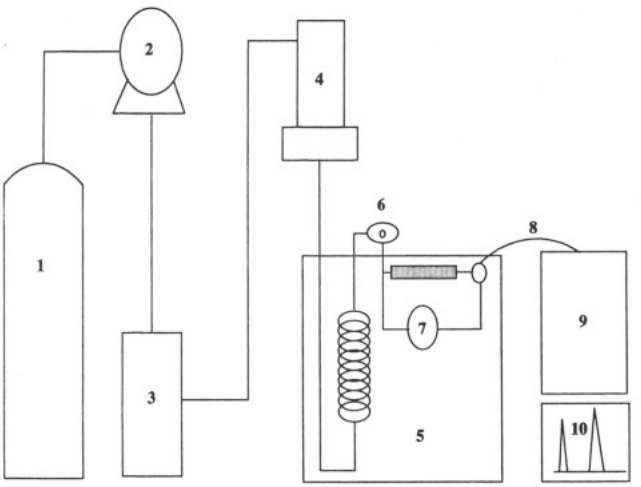

Figure 2. High-pressure chromatographic system: (1) gas cylinder, (2) gas booster, (3) high-pressure vessel, (4) syringe pump, (5) water bath, (6) injection valve, (7) differential pressure transducer, (8) heated restrictor, (9) light scattering detector, (10) recorder.

Table 1. Mole Fraction Solubility, S, and Capacity Factors, k_i, for C_7H_{16} in CH_4

T/K		P/ bar = 240	P/ bar = 200	P/ bar = 180	P/ bar = 160	P/ bar = 140	P/ bar = 120
423.2	10^1S	1.1	1.2	1.4	1.6	1.7	2.0
	k_i	0.49	0.49	0.49	0.49	0.50	0.51
393.2	10^1S	1.0	1.1	1.1	1.2	1.3	1.3
	k_i	0.43	0.46	0.52	0.53	0.55	0.63
358.2	10^2S	9.7	9.2	8.9	8.5	7.9	7.7
	k_i	0.49	0.56	0.63	0.73	0.87	1.03
348.2	10^2S	8.3	8.3	7.2	7.3	7.2	7.5
	k_i	0.53	0.62	0.78	0.87	1.01	1.11
338.2	10^2S	7.3	8.4	8.4	8.2	8.1	8.0
	k_i	0.55	0.56	0.61	0.71	0.82	0.96
328.2	10^2S	8.9	9.4	9.2	9.5	10.4	11.8
	k_i	0.41	0.45	0.51	0.55	0.57	0.60
318.2	10^2S	7.1	7.4	8.0	7.0	6.6	6.5
	k_i	0.46	0.52	0.53	0.67	0.80	0.97
308.2	10^2S	1.8	1.3	1.1	0.9	0.8	0.6
	k_i	0.51	0.70	0.84	0.95	1.15	1.39
298.2	10^2S	5.1	3.8	3.7	3.2	3.1	3.0
	k_i	0.52	0.79	0.90	1.16	1.39	1.69

Table 2. Mole Fraction Solubility, S, and Capacity Factors, k_i for C_8H_{18} in CH_4

T/K		P/ bar = 240	P/ bar = 200	P/ bar = 180	P/ bar = 160	P/ bar = 140	P/ bar = 120
423.2	10^2S	7.0	8.2	8.9	10.0	11.0	12.9
	k_i	0.7	0.8	0.8	0.8	0.8	0.8
393.2	10^2S	5.0	5.7	6.2	6.9	7.8	7.7
	k_i	0.9	0.9	0.9	0.9	0.9	1.1
358.2	10^2S	6.9	6.6	7.0	6.5	6.2	4.7
	k_i	0.7	0.8	0.8	1.0	1.1	1.7
348.2	10^2S	5.1	4.6	4.6	4.6	4.7	4.4
	k_i	0.9	1.1	1.2	1.4	1.6	1.9
338.2	10^2S	5.0	5.8	4.4	4.4	4.5	4.5
	k_i	0.8	0.8	1.2	1.3	1.5	1.7
328.2	10^2S	3.9	4.2	3.9	3.8	3.8	4.0
	k_i	1.0	1.0	1.2	1.4	1.6	1.8
318.2	10^2S	4.2	4.1	3.6	3.9	3.6	3.5
	k_i	0.8	0.9	1.2	1.2	1.5	1.8
308.2	10^2S	2.8	2.1	2.0	1.8	1.2	1.1
	k_i	1.0	1.6	1.9	2.4	3.9	5.0
298.2	10^2S	3.3	1.9	1.7	1.2	0.9	0.7
	k_i	0.8	1.6	2.0	3.0	4.8	7.1

temperature bath, controlled by a Bayley precision controller (BAYLEY 123). The bath was filled with water for the lower temperatures, or a heat transfer fluid (UCON 500) for the higher temperature studies. The fluid then enters an injection valve (VALCO CI4W1), where a 1 μL injection loop permits introduction of small amounts of the solute dissolved in pentane. Pentane was selected as the solvent, since it dissolved the solid hydrocarbons and was not retained in the packed column and its peak was detected each time, providing a reference measurement (t_o). The column (100 mm in length and 4.6 mm in internal diameter) was packed with 3 μm particles of HYPERSIL ODS C_{18} (ALLTECH C-6000B). The small pressure drop across the column (2–4 bar) is measured using a differential pressure transducer (VALYDINE CD12), while the system pressure is monitored with a pressure transducer and indicator (HEISE 901B). The effluent from the chromatographic column then flows through a deactivated silica tubing that acts as the restrictor (50 μm inside diameter and 40 cm length), where the fluid undergoes decompression. This restrictor is heated to compensate for the cooling effect from the Joule–Thompson expansion of the solvent, and to avoid deposition of the solutes along the restrictor during decompression.

Table 3. Mole Fraction Solubility, S, and Capacity Factors, k_i, for C_9H_{20} in CH_4

T/K		P/ bar = 240	P/ bar = 200	P/ bar = 180	P/ bar = 160	P/ bar = 140	P/ bar = 120
423.2	10^2S	5.1	5.8	6.3	7.2	7.9	8.9
	k_i	1.0	1.0	1.1	1.1	1.1	1.1
393.2	10^2S	3.9	4.3	4.3	4.5	4.5	4.4
	k_i	1.1	1.2	1.3	1.4	1.6	1.9
358.2	10^2S	4.2	4.2	4.2	3.9	3.6	3.5
	k_i	1.2	1.2	1.3	1.6	1.9	2.3
348.2	10^2S	3.5	3.8	3.8	3.4	3.6	3.2
	k_i	1.3	1.4	1.5	1.9	2.0	2.6
338.2	10^2S	2.9	2.8	2.2	2.3	2.2	2.1
	k_i	1.4	1.7	2.3	2.5	3.0	3.6
328.2	10^2S	2.1	2.4	2.3	2.0	1.9	1.9
	k_i	1.7	1.7	2.0	2.7	3.1	3.6
318.2	10^2S	2.0	1.8	1.6	1.2	1.0	0.8
	k_i	1.6	2.1	2.7	4.0	5.3	7.7
308.2	10^2S	1.7	1.2	1.1	0.9	0.8	0.7
	k_i	1.7	2.9	3.3	4.5	5.9	7.9
298.2	10^2S	1.7	1.0	0.9	0.6	0.5	0.4
	k_i	1.6	3.1	3.7	5.8	9.1	13.3

Table 4. Mole Fraction Solubility, S, and Capacity Factors, k_i, for $C_{10}H_{22}$ in CH_4

T/K		P/ bar = 240	P/ bar = 200	P/ bar = 180	P/ bar = 160	P/ bar = 140	P/ bar = 120
423.2	10^2S	3.7	4.3	4.6	4.9	4.5	5.2
	k_i	1.4	1.4	1.4	1.5	1.9	1.9
393.2	10^2S	2.5	2.8	2.6	2.9	2.7	2.7
	k_i	0.2	0.2	0.2	0.2	0.3	0.3
358.2	10^2S	2.6	2.5	2.6	2.7	2.3	2.1
	k_i	1.8	2.1	2.2	2.3	3.0	3.8
348.2	10^2S	2.2	2.3	2.4	2.5	1.9	1.9
	k_i	2.0	2.2	2.4	2.5	3.8	4.3
338.2	10^2S	1.8	1.5	1.3	1.1	1.0	0.9
	k_i	2.3	3.1	4.0	5.3	6.4	8.1
328.2	10^2S	1.5	1.2	1.1	1.0	0.9	0.8
	$10^{-1}k_i$	0.2	0.3	0.4	0.5	0.7	8.6
318.2	10^2S	1.3	1.1	1.0	0.9	0.6	0.5
	$10^{-1}k_i$	0.3	0.4	0.4	0.5	0.8	1.2
313.2	10^3S	8.8	5.4	4.0	3.0	2.3	1.8
	$10^{-1}k_i$	0.2	0.4	0.6	1.0	1.4	2.2
308.2	10^3S	9.9	6.6	5.8	4.8	4.0	3.4
	$10^{-1}k_i$	0.3	0.5	0.6	0.9	1.2	1.7
303.2	10^3S	7.2	4.5	3.4	2.6	1.9	1.4
	$10^{-1}k_i$	0.3	0.5	0.7	1.0	1.6	2.5
298.2	10^3S	8.1	5.5	4.8	3.8	3.1	2.6
	$10^{-1}k_i$	0.3	0.5	0.7	1.0	1.4	1.9
293.2	10^3S	6.3	4.1	3.3	2.6	2.1	1.7
	$10^{-1}k_i$	0.3	0.5	0.6	0.9	1.3	1.9

Table 5. Mole Fraction Solubility, S, and Capacity Factors, k_i, for $C_{11}H_{24}$ in CH_4

T/K		P/ bar = 240	P/ bar = 200	P/ bar = 180	P/ bar = 160	P/ bar = 140	P/ bar = 120
423.2	10^2S	3.1	3.0	3.2	3.4	3.2	3.2
	k_i	1.7	2.0	2.1	2.2	2.6	3.1
393.2	10^2S	1.8	1.6	1.7	1.9	1.8	1.7
	k_i	2.3	3.0	3.2	3.3	4.0	4.9
358.2	10^2S	1.6	1.6	1.5	1.5	1.4	1.4
	k_i	3.0	3.2	3.6	4.10	5.0	5.8
348.2	10^2S	1.4	1.5	1.5	1.5	1.3	1.3
	k_i	3.1	3.3	3.7	4.2	5.4	6.4
338.2	10^3S	10.9	9.0	7.2	5.6	5.1	4.5
	$10^{-1}k_i$	0.4	0.5	0.7	1.0	1.3	1.7
328.2	10^3S	10.3	7.6	6.6	5.1	5.8	6.6
	$10^{-1}k_i$	0.4	0.6	0.7	1.0	1.0	1.0
318.2	10^3S	8.3	7.0	6.5	5.2	4.2	3.4
	$10^{-1}k_i$	0.4	0.5	0.6	0.9	1.2	1.8
308.2	10^3S	6.3	4.0	3.8	3.1	2.6	2.2
	$10^{-1}k_i$	0.5	0.8	1.0	1.3	1.8	2.5
298.2	10^3S	5.6	3.3	2.7	1.9	1.4	1.1
	$10^{-1}k_i$	0.5	0.9	1.2	1.9	3.0	4.6

Table 6. Mole Fraction Solubility, S, and Capacity Factors, k_i, for $C_{12}H_{26}$ in CH_4

T/K		P/ bar = 240	P/ bar = 200	P/ bar = 180	P/ bar = 160	P/ bar = 140	P/ bar = 120
423.2	10^2S	2.2	2.3	2.3	2.3	1.9	2.1
	k_i	2.3	2.6	2.9	3.2	4.3	4.6
393.2	10^2S	1.3	1.2	1.2	1.2	1.1	1.0
	k_i	3.1	4.1	4.4	5.0	6.2	7.8
358.2	10^2S	1.1	0.9	0.9	0.8	0.7	0.6
	$10^{-1}k_i$	0.4	0.5	0.6	0.8	0.9	1.3
348.2	10^3S	8.7	8.7	7.9	7.3	6.6	5.8
	$10^{-1}k_i$	0.5	0.6	0.7	0.8	1.1	1.4
338.2	10^3S	7.4	5.7	4.4	3.6	3.1	2.7
	$10^{-1}k_i$	0.5	0.8	1.1	1.5	2.0	2.8
328.2	10^3S	6.8	4.5	4.1	3.3	3.5	3.9
	$10^{-2}k_i$	0.1	0.1	0.1	0.2	0.2	0.2
318.2	10^2S	0.5	0.5	0.4	0.3	0.3	2.0
	$10^{-1}k_i$	0.6	0.8	1.0	1.4	2.0	3.0
313.2	10^3S	3.6	1.8	1.4	0.9	0.7	0.5
	$10^{-1}k_i$	0.5	1.3	1.8	3.1	4.7	7.8
308.2	10^3S	3.9	2.4	2.5	1.9	1.6	1.4
	$10^{-1}k_i$	0.7	1.4	1.5	2.1	2.8	3.8
303.2	10^3S	2.8	1.5	1.1	0.7	0.5	0.4
	$10^{-1}k_i$	0.6	1.4	2.1	3.4	5.6	9.3
298.2	10^3S	3.2	1.6	1.6	1.2	0.9	0.7
	$10^{-1}k_i$	0.8	1.6	2.0	3.0	4.8	7.2
293.2	10^3S	2.3	1.3	0.9	0.7	0.5	0.3
	$10^{-1}k_i$	0.7	1.4	2.2	3.5	5.4	9.2

An important feature of the interface is the extension of the restrictor 1−2 mm into the evaporative chamber of the ELSD to act as the nebulizer. Other ELSD studies using liquid solvents (Carraud *et al.*, 1987; Nizeri *et al.*, 1989) have indicated the need for an additional heating step at the tip of the nebulizer to overcome additional crystallization of the mobile phase upon expansion. However, in this investigation the extra precaution was not required. In addition, the perfect vertical alignment of the restrictor/nebulizer inside the light scattering detector played an important role in the response.

Other researchers have reported that the use of a nebulizing gas (*i.e.*, N_2) might not be necessary for SCF applications (Carraud *et al.*, 1987; Nizeri *et al.*, 1989); however, our studies demonstrated better stability in the response (signal to noise ratio, S/N) when using such a nebulizing gas. The retention times used for this investigation were an average of several measurements obtained at the maxima of their response. The chromatographic column was maintained under pressure continuously to keep its performance (activity) constant. Since all solutions

Table 7. Mole Fraction Solubility, S, and Capacity Factors, k_i, for $C_{13}H_{28}$ in CH_4[a]

T/K		P/ bar = 240	P/ bar = 200	P/ bar = 180	P/ bar = 160	P/ bar = 140	P/ bar = 120
423.2	10^2S	1.7	1.8	1.6	1.6	1.2	1.4
	k_i	2.9	3.2	4.1	4.7	6.7	6.8
393.2	10^3S	9.3	8.1	8.2	8.0	7.3	7.3
	$10^{-1}k_i$	0.4	0.6	0.7	0.8	0.9	1.1
358.2	10^3S	6.7	6.2	5.0	4.4	4.2	4.2
	$10^{-1}k_i$	0.7	0.8	1.1	1.4	1.5	1.8
348.2	10^3S	6.0	5.0	4.0	3.8	4.1	4.0
	$10^{-1}k_i$	0.7	1.0	1.3	1.6	1.7	2.0
338.2	10^3S	4.6	3.5	2.7	2.3	2.0	1.7
	$10^{-1}k_i$	0.8	1.3	1.8	2.4	3.1	4.2
328.2	10^3S	4.4	2.8	2.7	2.1	2.2	2.3
	$10^{-1}k_i$	0.8	1.4	1.6	2.3	2.5	2.9
318.2	10^3S	3.4	2.8	2.7	2.0	1.6	1.3
	$10^{-1}k_i$	0.9	1.3	1.5	2.2	3.1	4.7
308.2	10^3S	2.5	1.5	1.4	1.0	0.8	0.7
	$10^{-1}k_i$	1.1	2.2	2.6	3.8	5.4	7.7
298.2	10^3S	1.4	1.1	1.0	0.6	0.5*	0.4*
	$10^{-2}k_i$	0.2	0.3	0.3	0.5	0.9*	1.3*

[a] An asterisk denotes extrapolated values.

Table 8. Mole Fraction Solubility, S, and Capacity Factors, k_i, for $C_{14}H_{30}$ in CH_4[a]

T/K		P/ bar = 240	P/ bar = 200	P/ bar = 180	P/ bar = 160	P/ bar = 140	P/ bar = 120
423.2	10^2S	1.1	1.2	1.1	1.1	0.9	0.9
	$10^{-1}k_i$	0.5	0.5	0.6	0.7	0.9	1.0
393.2	10^3S	5.8	6.2	5.7	5.4	5.5	4.7
	$10^{-1}k_i$	0.7	0.8	0.9	1.1	1.2	1.7
358.2	10^3S	4.7	3.9	3.2	2.6	2.5	2.5
	$10^{-1}k_i$	1.0	1.2	1.6	2.2	2.6	3.0
348.2	10^3S	4.0	3.8	3.6	3.4	3.4	3.1
	$10^{-1}k_i$	1.0	1.3	1.5	1.7	2.0	2.5
338.2	10^3S	2.9	2.3	1.7	1.6	1.4	1.2
	$10^{-1}k_i$	1.3	1.9	2.8	3.3	4.5	5.8
328.2	10^3S	2.9	1.8	1.6	1.2	1.3	1.4
	$10^{-1}k_i$	1.2	2.2	2.7	3.9	4.3	4.7
318.2	10^3S	2.1	1.9	1.8	1.2	1.0	0.7
	$10^{-1}k_i$	1.4	1.9	2.2	3.5	5.1	7.9
308.2	10^3S	1.6	0.9	0.9	0.6	0.5	0.4*
	$10^{-2}k_i$	0.2	0.4	0.4	0.6	0.9	1.3*
298.2	10^4S	8.6	6.6	5.9	3.6	2.5*	1.9*
	$10^{-2}k_i$	0.3	0.4	0.5	0.9	1.6*	2.4*

[a] An asterisk denotes extrapolated values.

studied were highly diluted, the densities used in the calculations were pure fluid densities obtained from Younglove and Ely (1987).

Chemicals

C.P. grade CH_4 (99.0% purity) was obtained from Matheson Gas Products. The n-alkanes from C_5H_{12} to $C_{36}H_{74}$ were obtained from Aldrich Chemical Co. with a stated purity of 98% or better. They were used without further purification since the chromatographic column separated out the impurities.

Results and Discussion

Tables 1−12 present experimental capacity factors and their corresponding calculated solubilities (eqs 4 and 5) for the n-alkanes from C_7H_{16} to $C_{18}H_{38}$ in CH_4 at temperatures from 293.2 to 423.2 K and pressures from 120 to 240 bar. Although C_5H_{12} and C_6H_{14} were also investigated, they flow unretained, or with a very small degree of retention through the chromatographic column.

The overall estimated experimental error in the measured capacity factors is approximately 5−10%, with the

Table 9. Mole Fraction Solubility, S, and Capacity Factors, k_i, for $C_{15}H_{32}$ in CH_4[a]

T/K		P/ bar = 240	P/ bar = 200	P/ bar = 180	P/ bar = 160	P/ bar = 140	P/ bar = 120
423.2	10^3S	8.6	9.4	8.0	6.4	6.3	6.6
	$10^{-1}k_i$	0.6	0.6	0.8	1.1	1.3	1.4
393.2	10^3S	4.0	4.3	3.7	3.6	3.6	3.3
	$10^{-1}k_i$	1.0	1.1	1.4	1.6	1.9	2.3
358.2	10^3S	3.4	2.5	1.9	1.6	1.6	1.5
	$10^{-1}k_i$	1.3	1.9	2.7	3.5	4.0	4.9
348.2	10^3S	2.6	2.5	2.3	2.1	2.1	2.0
	$10^{-1}k_i$	1.5	1.9	2.3	2.7	3.1	3.9
338.2	10^3S	1.7	1.3	1.2	0.9	0.8	0.7
	$10^{-2}k_i$	0.2	0.3	0.4	0.6	0.7	1.0
328.2	10^3S	2.3	1.2	1.1	0.9	0.7	0.8
	$10^{-1}k_i$	1.5	3.2	3.9	5.3	7.2	7.8
318.2	10^3S	1.3	1.2	1.1	0.8	0.6	0.5*
	$10^{-2}k_i$	0.2	0.3	0.3	0.6	0.8	1.2*
308.2	10^4S	9.6	5.3	4.4	2.7*	1.9*	1.8*
	$10^{-2}k_i$	0.3	0.6	0.8	1.4*	2.3*	2.9*
298.2	10^4S	7.2	4.0	3.3	2.0*	1.4*	1.0*
	$10^{-2}k_i$	0.3	0.7	0.9	1.7*	2.8*	4.4*

[a] An asterisk denotes extrapolated values.

Table 10. Mole Fraction Solubility, S, and Capacity Factors, k_i, for $C_{16}H_{34}$ in CH_4[a]

T/K		P/ bar = 240	P/ bar = 200	P/ bar = 180	P/ bar = 160	P/ bar = 140	P/ bar = 120
423.2	10^3S	6.9	6.5	5.6	4.4	4.4	5.1
	$10^{-1}k_i$	0.7	0.9	1.1	1.6	1.8	1.8
393.2	10^3S	3.1	3.0	2.8	1.9	2.5	2.0
	$10^{-1}k_i$	1.2	1.5	1.8	3.0	2.6	3.8
358.2	10^3S	2.6	2.0	1.3	1.0	1.0	0.9*
	$10^{-1}k_i$	1.7	2.4	4.1	5.6	6.1	8.1*
348.2	10^3S	1.7	1.6	1.5	1.4	1.4	1.2*
	$10^{-1}k_i$	2.3	2.9	3.5	4.2	4.8	6.0*
338.2	10^3S	1.0	0.9	0.9	0.6*	0.6*	0.6*
	$10^{-2}k_i$	0.4	0.5	0.5	0.8*	1.0*	1.2*
328.2	10^3S	1.4	0.9	0.6	0.5*	0.4*	0.5*
	$10^{-2}k_i$	0.2	0.4	0.7	0.9*	1.2*	1.3*
318.2	10^3S	0.9	0.8	0.7	0.5*	0.4*	0.3*
	$10^{-2}k_i$	0.3	0.4	0.5	0.9*	1.2*	1.8*
313.2	10^4S	6.7	3.0	1.8	1.1*	0.7*	0.4*
	$10^{-2}k_i$	0.3	0.7	1.3*	2.4*	4.1*	8.0*
308.2	10^4S	5.8	2.7	2.5*	1.8*	1.4*	1.4*
	$10^{-2}k_i$	0.4	1.1	1.3*	2.0*	3.1*	3.7*
303.2	10^4S	5.7	2.7	1.6*	1.0*	0.6*	0.4*
	$10^{-2}k_i$	0.3	0.7	1.3*	2.3*	4.2*	7.6*
298.2	10^4S	3.6	2.0	1.9*	1.1*	0.7*	0.6*
	$10^{-2}k_i$	0.6	1.3	1.5*	2.9*	5.0*	7.9*
293.2	10^4S	4.4	1.8	1.0*	0.6*	0.4*	0.2*
	$10^{-2}k_i$	0.3	0.9	1.8*	3.4*	6.3*	13.2*

[a] An asterisk denotes extrapolated values.

largest contributions (about 2–3% each) coming from the pressure drop across the column (2–4 bar), the flow variations from the constant pressure control (±0.2 mL/min), and the maxima of the retention times (±1–5 s). The error in the estimated solubilities is approximately 10–15%. The solvent density is known to 5% (Younglove and Ely, 1987), and the constant C_i is calculated with an estimated error of 10%. The large error in C_i is due to the inability to describe accurately the stationary phase. Although the solubility parameter of the stationary phase is regressed from one known solubility datum, the number obtained for an octadecyl bonded phase to a silica support (19.8 $MPa^{1/2}$) does not support that of octadecane (16.6 $MPa^{1/2}$). However, the bonded octadecyl is not expected to behave as a free octadecane molecule.

In order to verify the reliability of this approach, calculated solubilities for $C_{10}H_{22}$, $C_{12}H_{26}$, and $C_{16}H_{34}$ in CH_4 at 293.2 K were compared to those of Rijkers *et al.* (1992a,b, 1993) (Figure 3).

Table 11. Mole Fraction Solubility, S, and Capacity Factors, k_i, for $C_{17}H_{36}$ in CH_4[a]

T/K		P/ bar = 240	P/ bar = 200	P/ bar = 180	P/ bar = 160	P/ bar = 140	P/ bar = 120
423.2	10^3S	5.2	4.9	3.9	3.3	3.4	3.1
	$10^{-1}k_i$	0.9	1.1	1.5	2.1	2.3	3.0
393.2	10^3S	2.6	2.1	2.0	1.3	1.7	1.3
	$10^{-1}k_i$	1.5	2.1	2.5	4.2	3.7	5.8
358.2	10^3S	2.1	1.3	0.8	0.7	0.6	0.5*
	$10^{-2}k_i$	0.2	0.3	0.7	0.8	1.0	1.3*
348.2	10^3S	1.1	1.1	0.9*	0.8*	0.9*	0.8*
	$10^{-1}k_i$	3.4	4.3	5.4*	6.6*	7.4*	9.3*
338.2	10^4S	6.6	5.8	5.6*	3.6*	2.8*	2.4*
	$10^{-2}k_i$	0.5	0.7	0.8*	1.4*	2.1*	2.8*
328.2	10^4S	9.0	4.3	3.6*	3.0*	2.6*	2.9*
	$10^{-2}k_i$	0.4	0.8	1.1*	1.5*	2.0*	2.1*
318.2	10^4S	5.4	4.8	4.6*	2.8*	2.3*	1.9*
	$10^{-2}k_i$	0.5	0.7	0.8*	1.4*	2.0*	2.9*
308.2	10^4S	3.6	1.6*	1.4*	1.0*	0.8*	0.8*
	$10^{-3}k_i$	0.1	0.2*	0.2*	0.4*	0.5*	0.6*
298.2	10^4S	2.0*	1.2*	1.1*	0.6*	0.4*	0.3*
	$10^{-3}k_i$	0.1*	0.2*	0.3*	0.5*	0.9*	1.4*

[a] An asterisk denotes extrapolated values.

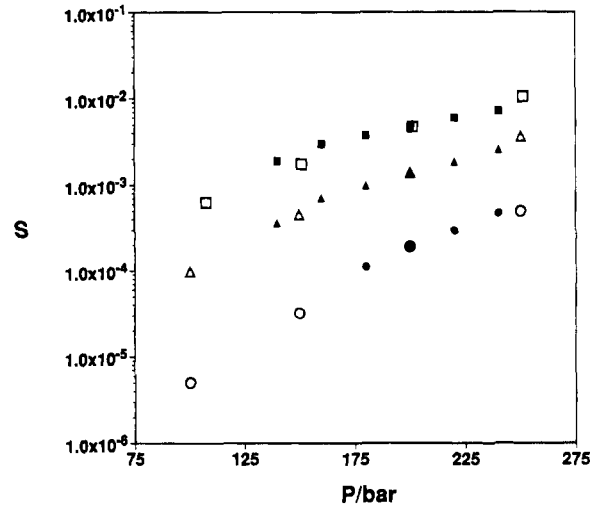

Figure 3. Mole fraction solubility, S, of various n-alkanes in CH_4 at 298.2 K: (□) $C_{10}H_{22}$, Rijkers *et al.* (1992a), (■) $C_{10}H_{22}$, this investigation, (△) $C_{12}H_{26}$, Rijkers *et al.* (1992b), (▲) $C_{12}H_{26}$, this investigation, (○) $C_{16}H_{34}$, Rijkers *et al.* (1993), (●) $C_{16}H_{34}$, this investigation.

For the high carbon number solutes at low temperatures, the elution time was too long to measure accurately (very low solubilities). However, because of the wealth of data available for other homologues, and the excellent linear relation between the log of the capacity factors and carbon number (Figure 4), it is possible to make excellent estimates of these capacity factors, and consequently solubilities. Tables 13–20 present capacity factors and the corresponding solubilities for the n-alkanes from $C_{20}H_{42}$ to $C_{36}H_{74}$ at 298.2–423.2 K and 120–240 bar. At the higher temperatures (*i.e.*, 423.2 and 393.2 K), the tables contain actual experimental data from $C_{20}H_{42}$ to $C_{28}H_{58}$, since the solutes eluted within a reasonable amount of time (*i.e.*, 1 h). However, most of the data presented in Tables 13–20 are extrapolated from the capacity factor versus carbon number correlations at each P and T. The extrapolated values are marked with an asterisk; the rest are actual experimental data.

In order to extract the solubility from the capacity factors for the solids, the ratio $P_{i,sub}/P_{i,vap}$ was required (eq 6).

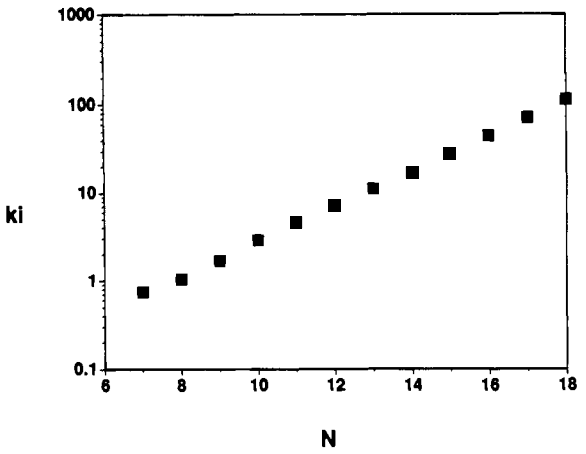

Figure 4. Capacity factors, k_i, versus carbon number, N, for the n-alkanes in CH_4 at 240 bar and 308.2 K.

Table 12. Mole Fraction Solubility, S, and Capacity Factors, k_i, for $C_{16}H_{38}$ in CH_4[a]

T/K		P/ bar = 240	P/ bar = 200	P/ bar = 180	P/ bar = 160	P/ bar = 140	P/ bar = 120
423.2	10^3S	4.3	3.6	2.5	2.3	2.1	2.5
	$10^{-1}k_i$	1.1	1.5	2.4	2.9	3.6	3.6
393.2	10^3S	1.9	1.5	1.4	1.0	1.2	0.8
	$10^{-2}k_i$	0.2	0.3	0.3	0.5	0.5	0.9
358.2	10^3S	1.6	0.9	0.5	0.4*	0.4*	0.3*
	$10^{-2}k_i$	0.3	0.5	0.9	1.3*	1.6*	2.2*
348.2	10^4S	7.5	6.9	5.8	5.3*	5.5*	5.0*
	$10^{-2}k_i$	0.5	0.6	0.8	1.0*	1.2*	1.4*
338.2	10^4S	4.1	3.5*	3.4*	2.2*	1.7*	1.4*
	$10^{-3}k_i$	0.1	0.1*	0.1*	0.2*	0.3*	0.5*
328.2	10^4S	6.0	2.6*	2.2*	1.8*	1.5*	1.7*
	$10^{-3}k_i$	0.1	0.1*	0.2*	0.2*	0.3*	0.4*
318.2	10^4S	3.4	3.1*	2.9*	1.7*	1.4*	1.2*
	$10^{-3}k_i$	0.1	0.1*	0.1*	0.2*	0.3*	0.4*
308.2	10^4S	2.2*	0.9*	0.8*	0.6*	0.4*	0.4*
	$10^{-3}k_i$	0.1*	0.3*	0.4*	0.6*	0.9*	1.1*
298.2	10^4S	1.1*	0.7*	0.6*	0.3*	0.2*	0.2*
	$10^{-3}k_i$	0.2*	0.4*	0.4*	0.9*	1.6*	2.6*

[a] An asterisk denotes extrapolated values.

Table 13. Mole Fraction Solubility, S, and Capacity Factors, k_i, for $C_{20}H_{42}$ in CH_4[a]

T/K		P/ bar = 240	P/ bar = 200	P/ bar = 180	P/ bar = 160	P/ bar = 140	P/ bar = 120
423.2	10^3S	2.6	1.9	1.2	1.2	1.1	1.2
	$10^{-1}k_i$	1.7	2.8	4.8	5.5	6.4	7.1
393.2	10^3S	1.1	0.7	0.7	0.5*	0.3*	0.3*
	$10^{-2}k_i$	0.3	0.6	0.6	1.2*	2.0*	2.0*
358.2	10^4S	5.6	3.2*	1.8*	1.3*	1.3*	1.1*
	$10^{-3}k_i$	0.1	0.1*	0.3*	0.4*	0.4*	0.6*
348.2	10^4S	3.3*	2.9*	2.3*	2.1*	2.2*	2.0*
	$10^{-3}k_i$	0.1*	0.1*	0.2*	0.2*	0.3*	0.3*
338.2	10^4S	1.6*	1.3*	1.3*	0.9*	0.6*	0.5*
	$10^{-3}k_i$	0.2*	0.3*	0.3*	0.5*	0.9*	1.2*
328.2	10^4S	2.6*	1.0*	0.8*	0.6*	0.5*	0.6*
	$10^{-3}k_i$	0.1*	0.3*	0.5*	0.7*	0.9*	1.0*
318.2	10^4S	1.3*	1.2*	1.2*	0.6*	0.6*	0.5*
	$10^{-3}k_i$	0.2*	0.2*	0.3*	0.6*	0.8*	1.1*
308.2	10^5S	8.2*	2.9*	2.6*	1.8*	1.3*	1.4*
	$10^{-3}k_i$	0.3*	0.9*	1.2*	1.8*	2.8*	3.1*
298.2	10^5S	1.4*	0.9*	0.9*	0.4*	0.3*	0.2*
	$10^{-4}k_i$	0.1*	0.1*	0.1*	0.3*	0.5*	0.8*

[a] An asterisk denotes extrapolated values.

Recent advances in the experimental measurement and prediction of $P_{i,sub}$ (Drake, 1993) and $P_{i,vap}$ (Morgan and Kobayashi, 1994) for the n-alkanes have allowed the accurate estimation of $P_{i,sub}/P_{i,vap}$, and subsequently the

Table 14. Mole Fraction Solubility, S, and Capacity Factors, k_i, for $C_{24}H_{50}$ in CH_4

T/K		P/ bar = 240	P/ bar = 200	P/ bar = 180	P/ bar = 160	P/ bar = 140	P/ bar = 120
423.2	10^3S	1.2*	0.5*	0.3*	0.2*	0.2*	0.2*
	$10^{-2}k_i$	0.3*	0.9*	1.9*	2.7*	3.2*	4.1*
393.2	10^4S	3.7*	2.6*	2.0*	0.7*	0.5*	0.6*
	$10^{-3}k_i$	0.1*	0.2*	0.2*	0.7*	1.0*	1.1*
358.2	10^4S	1.2*	0.5*	0.2*	0.2*	0.2*	0.1*
	$10^{-3}k_i$	0.3*	0.7*	1.7*	2.6*	3.1*	4.4*
348.2	10^5S	6.2*	5.2*	3.7*	3.2*	3.5*	3.1*
	$10^{-4}k_i$	0.1*	0.1*	0.1*	0.1*	0.2*	0.2*
338.2	10^5S	2.3*	1.9*	1.8*	1.3*	0.8*	0.7*
	$10^{-4}k_i$	0.1*	0.2*	0.2*	0.3*	0.6*	0.9*
328.2	10^5S	5.0*	1.3*	1.0*	0.8*	0.6*	0.7*
	$10^{-4}k_i$	0.1*	0.2*	0.3*	0.5*	0.7*	0.7*
318.2	10^6S	1.2*	1.2*	1.1*	0.5*	0.5*	0.4*
	$10^{-4}k_i$	0.1*	0.1*	0.2*	0.4*	0.5*	0.7*
308.2	10^6S	5.0*	1.3*	1.2*	0.8*	0.6*	0.6*
	$10^{-4}k_i$	0.2*	0.8*	1.0*	1.6*	2.6*	2.7*
298.2	10^7S	7.9*	4.9*	4.4*	1.9*	1.1*	0.7*
	$10^{-4}k_i$	0.4*	0.8*	1.0*	2.7*	5.2*	9.1*

[a] An asterisk denotes extrapolated values.

Table 15. Mole Fraction Solubility, S, and Capacity Factors, k_i, for $C_{28}H_{52}$ in CH_4[a]

T/K		P/ bar = 240	P/ bar = 200	P/ bar = 180	P/ bar = 160	P/ bar = 140	P/ bar = 120
423.2	10^4S	8.6*	3.9*	2.0*	1.5*	1.5*	1.3*
	$10^{-2}k_i$	0.5*	1.2*	2.6*	3.9*	4.6*	6.1*
393.2	10^4S	2.5*	1.4*	1.2*	0.4*	0.4*	0.4*
	$10^{-3}k_i$	0.1*	0.3*	0.4*	1.1*	1.5*	1.6*
358.2	10^5S	8.1*	3.5*	1.5*	1.1*	1.0*	0.8*
	$10^{-3}k_i$	0.4*	1.1*	2.7*	4.2*	5.1*	7.3*
348.2	10^5S	4.1*	3.4*	2.3*	2.0*	2.2*	1.9*
	$10^{-4}k_i$	0.1*	0.1*	0.2*	0.2*	0.2*	0.3*
338.2	10^5S	1.4*	1.2*	1.1*	0.8*	0.5*	0.4*
	$10^{-4}k_i$	0.2*	0.3*	0.3*	0.5*	0.9*	1.4*
328.2	10^5S	3.3*	0.8*	0.6*	0.5*	0.4*	0.4*
	$10^{-4}k_i$	0.1*	0.4*	0.5*	0.8*	1.1*	1.2*
318.2	10^6S	5.8*	5.6*	5.5*	2.3*	2.1*	1.8*
	$10^{-4}k_i$	0.2*	0.2*	0.2*	0.6*	0.7*	1.1*
308.2	10^6S	1.8*	0.4*	0.4*	0.3*	0.2*	0.2*
	$10^{-4}k_i$	0.3*	1.3*	1.7*	2.7*	4.6*	4.6*
298.2	10^7S	2.6*	1.6*	1.4*	0.6*	0.3*	0.2*
	$10^{-4}k_i$	0.1*	0.1*	0.2*	0.5*	0.9*	1.6*

[a] An asterisk denotes extrapolated values.

prediction of solubilities for the heavier solids. The solubilities for these heavy compounds are so small (ppm and even ppb) that measurements by conventional methods (*e.g.*, transpiration techniques) could not be used to verify these results. However, the different trends in the solubility of the even- and odd-numbered solid n-alkanes are similar to those observed by Moradinia and Teja in ethane (Moradinia and Teja, 1986, 1987, 1988).

Since the experimentally determined capacity factors are proportional to Φ_i^∞ (eq 3), second virial coefficients, B_{12}, were obtained for the n-alkanes in CH_4. The results compared well to those available in the literature (Dymond and Smith, 1980). For example, B_{12} for $C_{10}H_{22}$ in CH_4 from this investigation was -312 ± 20 cm^3/mol at 313 K, while Dymond and Smith tabulated -289 ± 10 cm^3/mol at 323 K. It was also noted that, although a single second virial coefficient was not sufficient to accurately describe Φ_i^∞, the inaccuracy of the higher order coefficients does not justify their use.

Partial Molar Volumes and Enthalpies

The density derivative of the capacity factors can be used to obtain partial molar volumes at infinite dilution, $\bar{V}_i^\infty$ (van

Table 16. Mole Fraction Solubility, S, and Capacity Factors, k_i, for $C_{28}H_{58}$ in CH_4[a]

T/K		P/bar = 240	P/bar = 200	P/bar = 180	P/bar = 160	P/bar = 140	P/bar = 120
423.2	10^5S	46.8	15.1*	6.7*	4.8*	4.6*	3.8*
	$10^{-3}k_i$	0.1	0.3*	0.7*	1.2*	1.4*	2.0*
393.2	10^5S	15.6*	4.6*	3.9*	1.2*	1.0*	1.0*
	$10^{-3}k_i$	0.2*	0.8*	1.0*	3.8*	5.1*	5.8*
358.2	10^6S	25.1*	9.4*	3.5*	2.4*	2.1*	1.7*
	$10^{-4}k_i$	0.1*	0.4*	1.1*	1.8*	2.3*	3.2*
348.2	10^6S	11.6*	9.4*	5.9*	5.0*	5.5*	4.8*
	$10^{-4}k_i$	0.3*	0.4*	0.6*	0.9*	0.9*	1.2*
338.2	10^6S	3.4*	2.7*	2.5*	1.9*	1.1*	0.9*
	$10^{-4}k_i$	0.8*	1.2*	1.4*	2.0*	4.0*	6.0*
328.2	10^7S	9.4*	1.8*	1.3*	1.0*	0.7*	0.8*
	$10^{-4}k_i$	0.2*	1.5*	2.2*	3.3*	5.1*	5.4*
318.2	10^7S	8.3*	8.3*	8.3*	3.1*	2.9*	2.4*
	$10^{-4}k_i$	0.6*	0.7*	0.8*	2.4*	2.9*	4.2*
308.2	10^7S	2.9*	0.6*	0.5*	0.3*	0.2*	0.3*
	$10^{-5}k_i$	0.1*	0.6*	0.9*	1.4*	2.5*	2.3*
298.2	10^8S	3.5*	2.2*	1.9*	0.0*	0.4*	0.2*
	$10^{-5}k_i$	0.4*	0.7*	0.8*	2.5*	5.3*	9.7*

[a] An asterisk denotes extrapolated values.

Table 17. Mole Fraction Solubility, S, and Capacity Factors, k_i, for $C_{29}H_{60}$ in CH_4[a]

T/K		P/bar = 240	P/bar = 200	P/bar = 180	P/bar = 160	P/bar = 140	P/bar = 120
423.2	10^5S	3.7*	1.1*	0.5*	0.3*	0.3*	0.3*
	$10^{-3}k_i$	0.1*	0.4*	1.1*	1.7*	2.0*	2.9*
393.2	10^5S	8.0*	3.2*	2.7*	0.8*	0.7*	0.7*
	$10^{-3}k_i$	0.4*	1.1*	1.4*	5.7*	7.6*	8.8*
358.2	10^6S	1.7*	0.6*	0.2*	0.1*	0.1*	0.1*
	$10^{-6}k_i$	0.2*	0.6*	1.8*	2.8*	3.7*	5.4*
348.2	10^6S	7.6*	6.1*	3.7*	3.1*	3.5*	3.0*
	$10^{-5}k_i$	0.4*	0.6*	1.0*	1.3*	1.4*	1.8*
338.2	10^6S	2.1*	1.7*	1.5*	1.2*	0.7*	0.5*
	$10^{-5}k_i$	0.1*	0.2*	0.2*	0.3*	0.6*	1.0*
328.2	10^7S	3.7*	0.6*	0.5*	0.4*	0.3*	0.3*
	$10^{-6}k_i$	0.4*	2.5*	3.6*	5.4*	8.5*	9.0*
318.2	10^8S	8.1*	8.1*	8.2*	2.9*	2.7*	2.3*
	$10^{-5}k_i$	0.1*	0.1*	0.1*	0.4*	0.5*	0.7*
308.2	10^8S	10.1*	2.0*	1.6*	1.1*	0.7*	0.9*
	$10^{-6}k_i$	0.2*	1.1*	1.5*	2.4*	4.3*	4.0*
298.2	10^9S	11.0*	6.9*	6.1*	2.1*	1.1*	0.7*
	$10^{-6}k_i$	0.1*	0.1*	0.1*	0.4*	0.9*	1.8*

[a] An asterisk denotes extrapolated values.

Table 18. Mole Fraction Solubility, S, and Capacity Factors, k_i, for $C_{32}H_{66}$ in CH_4[a]

T/K		P/bar = 240	P/bar = 200	P/bar = 180	P/bar = 160	P/bar = 140	P/bar = 120
423.2	10^5S	16.3*	4.2*	1.5*	1.0*	1.0*	0.7*
	$10^{-4}k_i$	0.2*	1.0*	3.0*	5.2*	5.9*	9.3*
393.2	10^5S	3.2*	1.1*	0.9*	0.2*	0.2*	0.2*
	$10^{-3}k_i$	0.9*	3.1*	4.0*	19.7*	25.5*	30.7*
358.2	10^6S	5.3*	1.6*	0.5*	0.3*	0.3*	0.2*
	$10^{-4}k_i$	0.6*	2.0*	7.2*	11.8*	16.4*	24.0*
348.2	10^6S	2.2*	1.7*	0.9*	0.8*	0.9*	0.8*
	$10^{-4}k_i$	1.2*	1.9*	3.7*	5.0*	5.1*	6.7*
338.2	10^7S	9.3*	7.2*	6.5*	5.2*	2.7*	2.1*
	$10^{-5}k_i$	0.5*	0.7*	0.9*	1.3*	2.7*	4.2*
328.2	10^7S	16.6*	2.2*	1.6*	1.2*	0.8*	0.9*
	$10^{-5}k_i$	0.1*	1.0*	1.5*	2.3*	3.9*	4.1*
318.2	10^8S	13.4*	13.9*	14.1*	4.4*	4.3*	3.6*
	$10^{-5}k_i$	0.4*	0.4*	0.4*	1.6*	1.8*	2.5*
308.2	10^9S	35.1*	5.5*	4.5*	3.0*	2.8*	2.5*
	$10^{-5}k_i$	0.7*	5.5*	7.4*	12.3*	15.5*	19.9*
298.2	$10^{10}S$	31.7*	19.7*	17.6*	5.3*	2.8*	1.7*
	$10^{-6}k_i$	0.3*	0.5*	0.7*	2.4*	5.4*	10.5*

[a] An asterisk denotes extrapolated values.

Table 19. Mole Fraction Solubility, S, and Capacity Factors, k_i, for $C_{33}H_{68}$ in CH_4[a]

T/K		P/bar = 240	P/bar = 200	P/bar = 180	P/bar = 160	P/bar = 140	P/bar = 120
423.2	10^5S	12.8*	3.1*	1.1*	0.7*	0.7*	0.5*
	$10^{-3}k_i$	0.3*	1.3*	4.3*	7.5*	8.5*	13.7*
393.2	10^5S	2.4*	0.7*	0.6*	0.1*	0.1*	0.1*
	$10^{-4}k_i$	0.1*	0.4*	0.6*	3.0*	3.8*	4.7*
358.2	10^6S	3.6*	1.0*	0.3*	0.2*	0.2*	0.1*
	$10^{-5}k_i$	0.1*	0.3*	1.2*	1.9*	2.7*	3.9*
348.2	10^6S	1.4*	1.1*	0.6*	0.5*	0.5*	0.5*
	$10^{-5}k_i$	0.2*	0.3*	0.6*	0.8*	0.8*	1.0*
338.2	10^6S	0.4*	0.3*	0.3*	0.2*	0.1*	0.1*
	$10^{-5}k_i$	0.8*	1.2*	1.4*	2.0*	4.4*	6.8*
328.2	10^7S	7.5*	0.9*	0.7*	0.5*	0.3*	0.4*
	$10^{-5}k_i$	0.2*	1.6*	2.4*	3.8*	6.4*	6.7*
318.2	10^7S	1.1*	1.2*	1.2*	0.4*	0.3*	0.3*
	$10^{-5}k_i$	0.6*	0.6*	0.7*	2.5*	2.9*	4.0*
308.2	10^8S	1.4*	0.2*	0.2*	0.1*	0.1*	0.1*
	$10^{-6}k_i$	0.1*	0.9*	1.3*	2.1*	2.2*	3.4*
298.2	10^9S	1.2*	0.7*	0.6*	0.2*	0.1*	
	$10^{-6}k_i$	0.5*	0.9*	1.1*	4.2*	9.6*	18.9*

[a] An asterisk denotes extrapolated values.

Wasen *et al.*, 1980; Shim and Johnston, 1991):

$$\bar{V}_i^{\infty} = V_i + RT\kappa_T\left|1 + \varrho\left|\frac{\partial \ln(k_i)}{\partial \varrho}\right|_T\right| \quad (7)$$

where κ_T is the isothermal compressibility $(1/\varrho)(d\varrho/dP)_T$ and ϱ is the solvent density.

This approach has proven to be extremely useful for obtaining $\bar{V}_i^{\infty}$, since other experimental techniques for obtaining such properties (*e.g.*, precise density measurements, constant volume measurements, and measurements of volume changes upon mixing) (Eckert *et al.*, 1986; Foster *et al.*, 1989) may require long times for each measurement (*i.e.*, 12 h), and extremely precise measurements.

Similarly, the temperature derivative of the capacity factors can be used to obtain the partial molar enthalpy at infinite dilution, $\bar{H}_i^{\infty}$ (Shim and Johnston, 1991):

$$\bar{H}_i^{\infty} = H_i^{L} - RT^2\left|\left|\frac{\partial \ln(k_i)}{\partial T}\right|_P - \beta\right| \quad (8)$$

H_i^{L} is the molar enthalpy of the pure (subcooled) liquid, and β is the volume expansivity $-(1/\varrho)(d\varrho/dT)_P$.

These derivative properties are extremely useful for developing and testing theories/models describing the phase equilibrium behavior of SCFs, as well as for understanding the behavior of mixtures at the molecular level. These properties have been closely studied in the vicinity of the critical point of the solvent, since in this region both $\bar{V}_i^{\infty}$ and $\bar{H}_i^{\infty}$ go through a minimum or maximum (Eckert *et al.*, 1986; Foster *et al.*, 1989; Abraham and Ehrlich, 1973; Khazanova and Saminskaya, 1968), indicative of the attractive or repulsive forces between unlike molecules. As one moves away from the critical point, one expects this dynamic situation to stabilize, and the $\bar{V}_i^{\infty}$ and $\bar{H}_i^{\infty}$ values to level off, approaching constant values (*i.e.*, $\bar{V}_i^{\infty} = V_i$).

This investigation was performed removed from the critical point of methane (T_c = 190.6 K, P_c = 46.0 bar), and although there are no large variations in the $\bar{V}_i^{\infty}$ and $\bar{H}_i^{\infty}$ results, they provided additional manifestations of the strong dispersion forces between these paraffinic molecules.

Figure 5 presents $\bar{V}_i^{\infty}$ for $C_{10}H_{22}$ in CH_4 at 313.2 K. The values of Rijkers *et al.* (1992a) were obtained from the method developed by Kumar and Johnston (Kumar and Johnston, 1988). There are two interesting features from

Table 20. Mole Fraction Solubility, S, and Capacity Factors, k_i, for $C_{36}H_{74}$ in CH_4[a]

T/K		P/ bar = 240	P/ bar = 200	P/ bar = 180	P/ bar = 160	P/ bar = 140	P/ bar = 120
423.2	10^6S	61.0*	12.0*	3.5*	2.2*	2.1*	1.5*
	$10^{-3}k_i$	0.6*	3.3*	12.0*	23.0*	26.0*	44.0*
393.2	10^6S	9.7*	2.4*	2.1*	0.4*	0.3*	0.3*
	$10^{-4}k_i$	0.3*	1.3*	1.6*	10.0*	13.0*	16.0*
358.2	10^7S	11.0*	2.7*	0.7*	0.4*	0.3*	0.3*
	$10^{-4}k_i$	2.4*	10.6*	46.8*	79.0*	118.9*	176.7*
348.2	10^7S	4.0*	3.0*	1.5*	1.2*	1.4*	1.2*
	$10^{-4}k_i$	5.9*	9.4*	20.8*	29.4*	28.9*	38.4*
338.2	10^8S	12.5*	9.4*	8.4*	7.1*	3.4*	2.4*
	$10^{-5}k_i$	3.0*	4.7*	5.7*	7.7*	18.4*	29.5*
328.2	10^7S	2.9*	0.3*	0.2*	0.1*	0.1*	0.1*
	$10^{-4}k_i$	5.5*	67.2*	103.7*	163.0*	251.0*	304.3*
318.2	10^8S	2.7*	3.0*	3.1*	0.8*	0.8*	0.7*
	$10^{-5}k_i$	2.0*	2.2*	2.4*	10.2*	11.3*	15.6*
308.2	10^9S	4.2*	0.5*	0.4*	0.3*	0.2*	0.2*
	$10^{-5}k_i$	4.7*	45.8*	63.8*	108.7*	148.1*	170.7*
298.2	$10^{10}S$	2.9*	1.8*	1.6*	0.4*	0.2*	0.1*
	$10^{-6}k_i$	2.3*	4.3*	5.3*	23.0*	54.7*	112.1*

[a] An asterisk denotes extrapolated values.

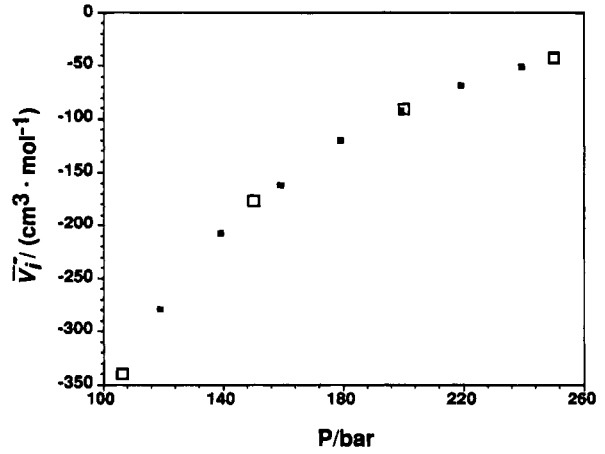

Figure 5. $\bar{V}_i^\infty$ for $C_{10}H_{22}$ in CH_4 at 313.2 K: (□) Rijkers *et al.* (1992a), (■) this investigation.

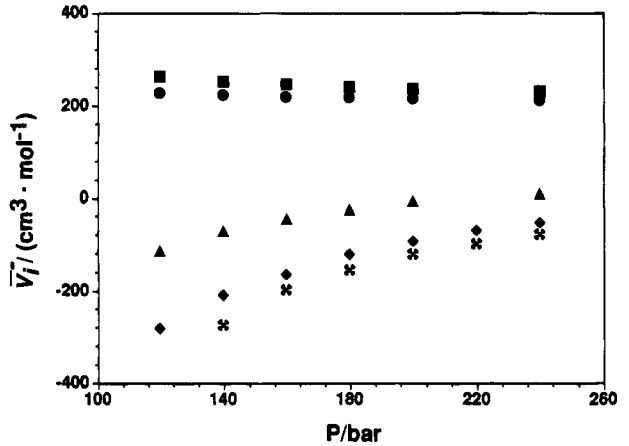

Figure 6. $\bar{V}_i^\infty$ for $C_{10}H_{22}$ in CH_4 at various temperatures: (■) 423.2 K, (●) 393.2 K, (▲) 358.2 K, (♦) 313.2 K, (*) 293.2 K.

these results: First, the negative $\bar{V}_i^\infty$ values show strong solvent–solute interactions, even though this investigation was performed more than 100 K above the solvent's critical temperature. Second is the fact that these forces are more significant at the lower pressures where the solvent density is more gaslike.

Figure 6 presents $\bar{V}_i^\infty$ for $C_{10}H_{22}$ in CH_4 at various temperatures. At the higher temperatures $\bar{V}_i^\infty$ approaches

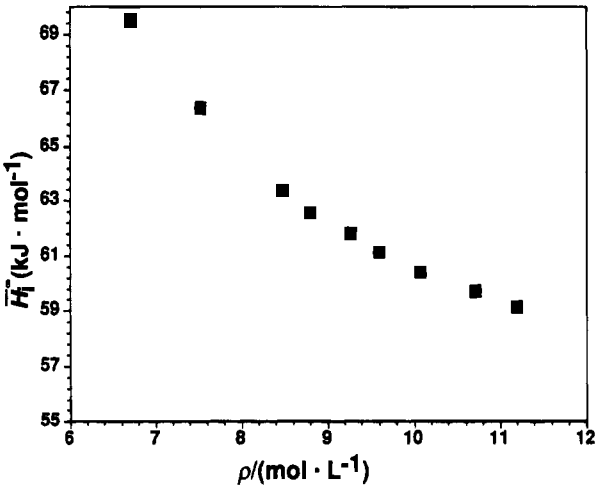

Figure 7. $\bar{H}_i^\infty$ for $C_{10}H_{22}$ in CH_4.

V_i (196 cm^3/mol). However, at the lower temperatures the $\bar{V}_i^\infty$ is smaller than V_i, indicative of strong attractive forces between unlike molecules.

The effect of temperature in the phase equilibria of the alkanes is best described by the $\bar{H}_i^\infty$. Figure 7 presents the $\bar{H}_i^\infty$ for $C_{10}H_{22}$ in CH_4. These endothermic results are in accord with the higher solubilities at higher temperatures. At lower pressures the increase of $\bar{H}_i^\infty$ also agrees with the picture presented by $\bar{V}_i^\infty$ of increasing local density or clustering. The solvation picture is supported by the limited virial coefficient information in methane (Dymond and Smith, 1980).

Looking at the n-alkanes, as the solute carbon number increases, $V_i^\infty - \bar{V}_i^\infty$ and $\bar{H}_i^\infty - H_i^L$ increase. This point indicates that as the solute carbon number increases, the solute is solvated more strongly, and therefore the energy of interaction between the alkanes and methane increases. Note that $(\bar{H}_i^\infty - H_i^L)$ is the molar energy required to dissolve a single pure subcooled liquid solute molecule in methane gas solvent. This energy increase implies that when modeling these systems, the enthalpic contribution should also be considered.

To conclude the analysis of these derivative properties, it is important to emphasize that these results should be considered on a qualitative basis only. Although an extensive evaluation of the temperature and density dependence of the capacity factors was performed for this investigation, these derivative properties are extremely sensitive to errors in the data. A very small change in the solubility versus density plot will provide a drastic shift in the $\bar{V}_i^\infty$ (Figure 8). It is always superior to measure a derivative property directly than to differentiate an integral property.

Conclusions

In conclusion, a chromatographic technique for the fast and accurate measurement of capacity factors for n-alkanes in SCFs/dense gases is presented. The technique determines solubilities, virial coefficients, partial molar volumes, and partial molar enthalpies at infinite dilution from the chromatographic capacity factors. A database of capacity factors and their corresponding solubilities is presented from C_7H_{16} to $C_{36}H_{74}$ in CH_4. Future communications will use the described method to present phase equilibrium data for the n-alkanes in other gases and mixtures.

Acknowledgment

We thank Steven J. Waxmonsky, Steven P. Girardot, and Frank A. Crumpler for taking part of the data for this

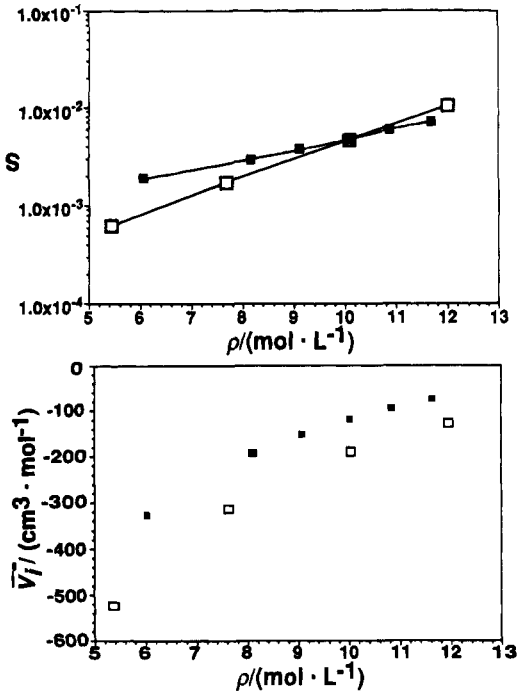

Figure 8. Solubility, S, and $\bar{V}_i^\infty$ of $C_{10}H_{22}$ in CH_4 at 293.2 K: (□) Rijkers *et al.* (1992a), (■) this investigation.

investigation. The discussions with Frederic Pouillot and Martin S. Schiller regarding the prediction of solubilities from chromatographic capacity factors are very much appreciated. We also acknowledge the discussions with Professor Amyn S. Teja and Vicky Smith.

Nomenclature

B_{12}	second virial coefficient
$C_i(T)$	constant for a particular solute, chromatographic column, and temperature, T
H_i^L	molar enthalpy of the pure (subcooled) liquid
$\bar{H}_i^\infty$	partial molar enthalpy at infinite dilution
$k_{H,i}$	Henry's constant of solute i in the stationary phase
$k°_{H,i}$	Henry's constant for solute i in the stationary phase at the reference pressure, $P°$ ($k°_{H,i} = P_{i,vap}\,\gamma_i^\infty$)
k_i	chromatographic capacity factor
P	pressure
$P°$	reference pressure
$P_{i,sat}$	saturation (vapor/sublimation) pressure of solute i
$P_{i,sub}$	sublimation pressure of solute i
$P_{i,vap}$	vapor pressure of solute i
R	universal gas constant
T	temperature
t_i	retention time of solute i
t_o	retention time of an unretained solvent
V^m	physical volume of the mobile phase inside the chromatographic column
V^s	physical volume of the stationary phase
V_m^m	molar volume of the mobile phase
V_m^s	molar volume of the stationary phase
V_i	molar volume of solute i
$\bar{V}_i^\infty$	partial molar volume of solute i at infinite dilution
$\bar{V}_i$	partial molar volume of solute i in the stationary phase
x_i	mole fraction of solute i in the stationary phase
y_i	mole fraction of solute i in the mobile phase (solubility)

Greek Letters

β	volume expansivity, $-(1/\varrho)(d\varrho/dT)$
κ	isothermal compressibility, $(1/\varrho)(d\varrho/dP)$
γ_i^∞	infinite dilution activity coefficient of solute i in the stationary phase
Φ_i^∞	fugacity coefficient of solute i in the mobile phase at infinite dilution

Superscripts

∞	infinitely diluted
m	mobile phase
o	reference state
s	stationary phase

Literature Cited

Abraham, K. P.; Ehrlich, P. Partial Molar Volume of a Polymer in Supercritical Solution. *Macromolecules* **1975**, *8*, 944–946.

Abraham, M. H.; Whiting, G. S.; Fuchs, R.; Chambers, E. J. Thermodynamics of Solute Transfer from Water to Hexadecane. *J. Chem. Soc., Perkin Trans.* **1990**, *2*, 291–300.

Arai, K.; Chen, R. J. J.; Kobayashi, R. Prediction of the Dew Point Locus in Methane-Light Hydrocarbon Binary Systems in the Neirborhood of the Methane Critical Point. *AIChE J.* **1974**, *20*, 399–401.

Arai, K.; Kobayashi, R. Interpretation of the Isochoric P-V-T Behavior of a Nominal 95 Mole % Methane 5 Mole % Propane Mixture from Near Ambient to Cryogenic Temperatures. *Adv. Cryog. Eng.* **1980**, *25*, 640–653.

Barker, I. K.; Bartle, K. D.; Clifford, A. A. Measurement of Solubilities in Fluids at Supercritical Temperatures and Lower Pressures Using Chromatographic Retention. *Chem. Eng. Commun.* **1988**, *68*, 177–184.

Bartle, K. D.; Clifford, A. A.; Jafar, S. A. Relationship Between Retention of a Solid Solute in Liquid and Supercritical Fluid Chromatography and its Solubility in the Mobile Phase. *J. Chem. Soc., Faraday Trans.* **1990a**, *86*, 855–860.

Bartle, K. D.; Clifford, A. A.; Jafar, S. A. Measurement of Solubility in Supercritical Fluids Using Chromatographic Retention: The Solubility of Fluorene, Phenanthrene, and Pyrene in Carbon Dioxide. *J. Chem. Eng. Data* **1990b**, *35*, 355–360.

Brown, B. O.; Kishbaugh, A. J.; Paulaitis, M. E. Experimental Determination of Enhancement Factors from Supercritical-Fluid Chromatography. *Fluid Phase Equilib.* **1987**, *36*, 247–261.

Carraud, P.; Thiebaut, O.; Claude, M.; Rosset, R.; Lafosse, M.; Dreux, M. Supercritical Fluid Chromatography/Light-Scattering Detector: A Promising Coupling for Polar Compounds Analysis with Packed Columns. *J. Chromatogr. Sci.* **1987**, *25*, 395–398.

Chen, R. J. J.; Ruska, W. J. A.; Chappelear, P. S.; Kobayashi, R. Development of a Method for the Direct Determination of Dew Point Loci of Methane-heavier Hydrocarbon Mixtures at Low Temperatures and Elevated Pressures. *Adv. Cryog. Eng.* **1973**, *18*, 202–207.

Cheong, W. J. Measurements of Limiting Activity Coefficients of Homologous Series of Solutes and their Application to the Study of Retention Mechanism. Ph.D. Thesis, University of Minnesota, 1989.

D'Avila, S, G.; Kaul, B. K.; Prausnitz, J. M. Solubilities of Heavy Hydrocarbons in Compressed Methane and Nitrogen. *J. Chem. Eng. Data* **1976**, *21*, 488.

Drake, B. D. Prediction of Sublimation Pressures of Low Volatility Solids Ph.D. Thesis, Universtiy of South Carolina, 1993.

Dymond, J. H.; Smith, E. B. *The Virial Coefficients of Pure Gases and Mixtures. A Critical Compilation*; Oxford University Press: New York, 1980.

Eckert, C. A.; Ziger, D. H.; Johnston, K. P.; Kim, S. Solute Partial Molal Volumes in Supercritical Fluids. *J. Phys. Chem.* **1986**, *90*, 2738–2746.

Eikens, D. Applicability of Theoretical and Semi-empirical Models for Predicting Infinite Dilution Activity Coefficients. Ph.D. Thesis, University of Minnesota, 1993.

Ekart, M. P.; Bennett, K. L.; Ekart, S. M.; Gurdial, G. S.; Liotta, C. L.; Eckert C. A. Cosolvent Interactions in Supercritical Fluid Solutions. *AIChE J.* **1992**, *39*, 235–248.

Ekart, M. P.; Bennett, K. L.; Eckert, C. A. Effects of Specific Interactions in Supercritical Fluid Solutions: A Chromatographic Study. *ACS Symp. Ser.* **1993**, *514*, 228–235.

Fedors, R. F. A Method for Estimating Both the Solubility Parameters and Molar Volumes of Liquids. *Polym. Eng. Sci.* **1974**, *14*, 147.

Foster, N. R.; Macnaughton, S. J.; Chaplin, R. P.; Wells, T. Critical Locus and Partial Molar Volume Studies of the Benzaldehyde-Carbon Dioxide Binary System. *Ind. Eng. Chem. Res.* **1989**, *28*, 1903–1907.

Henry, D. L.; Evans, L. E.; Kobayashi, R. Evidence for a Background Contribution to the Decay Rate of ConcentrationFluctuations in Ethane + Propane Near the Critical Point. *J. Chem. Phys.* **1977**, *66*, 1802–1807.

Hildebrand, J. H.; Prausnitz J. M.; Scott, R. L., *Regular and Related Solutions; The Solubility of Gases, Liquids, and Solids;* van Nostrand Reinhold Co.: New York, 1970.

Johnston, K. P.; Eckert, C. A. An Analytical Carnahan-Starling-van der Waals Model for the Solubility of Hydrocarbon Solids in Supercritical Fluids. *AIChE J.* **1981**, *27*, 773–779.

Johnston, K. P.; Ziger, D. H.; Eckert, C. A. Solubilities of Hydrocarbon Solids in Supercritical Fluids. The Augmented van der Waals Treatment. *Ind. Eng. Chem. Fundam.* **1982**, *21*, 191–197.

Kaul, B. K.; Prausnitz, J. M. Solubilities of Heavy Hydrocarbons in Compressed Methane, Ethane, and Ethylene: Dew-Point Temperatures for Gas Mixtures Containing Small and Large Molecules. *AIChE J.* **1978**, *24*, 223.

Khazanova, N. E.; Saminskaya, E. E.; Volume Properties of Binary Gaseous Solutions Close to the Critical Pressures and Temperatures of the Pure Components. *Russ. J. Phys. Chem.* **1968**, *42*, 676–682.

Kumar, S. K.; Johnston, K. P. Modeling the Solubility of Solids in Supercritical Fluids with Density as the Independent Variable. *J. Supercrit. Fluids* **1988**, *1*, 15–22.

Magee, J. W.; Arai, K.; Kobayashi, R. Interpretation of the Isochoric P-V-T Behavior of a Nominal 95 Mole % Methane 5 Mole % Propane Mixture from Near ambient to Cryogenic Temperatures. *Adv. Cryog. Eng.* **1982**, *27*, 869–874.

Moradinia, I; Teja, A. S. Solubilities of Solid n-Octacosane, n-Triacontane and n-Dotriacontane in Supercritical Ethane. *Fluid Phase Equilib.* **1986**, *28*, 199–209.

Moradinia, I.; Teja, A. S. Solubilities of Five Solid n-alkanes in Supercritical Ethane. *Supercrit. Fluids ACS Symp. Ser.* **1987**, *329*, 130–137.

Moradinia, I.; Teja, A. S. Solubilities of Solid n-Nonacosane and n-Tritriacontane in Supercritical Ethane. *J. Chem. Eng. Data* **1988**, *33*, 240–242.

Morgan, D. L.; Kobayashi, R. Direct Vapor Pressure Measurements of Ten n-Alkanes in the C_{10} to C_{28} Range. *Fluid Phase Equilib.* **1994**, *97*, 211–242.

Nizeri, D.; Thiebaut, D.; Claude, M.; Rosset, R. Improved Evaporative Light Scattering Detection for Supercritical Fluid Chromatography with Carbon Dioxide-Methanol Mobile Phases *J. Chromatogr.* **1989**, *467*, 49–60.

Olds, R. H.; Sage, B. H.; Lacey, W. N. Methane-Isobutane System. *Ind. Eng. Chem. Ind. Ed.* **1942**, *34*, 1008.

Park, J. H. Headspace Gas Chromatographic Measurement and Applications of Limiting Activity Coefficients. Ph.D. Thesis, University of Minnesota, 1988.

Prausnitz, J. M.; Lichtenthaler, R. N.; Gomes de Azevedo, E. *Molecular Thermodynamics of Fluid Phase Equilibria*; Prentice-Hall: Englewood Cliffs, NJ, 1986.

Reamer, H. H.; Korpi, K. J.; Sage, B. H.; Lacey, W. N. Phase Equilibria in Hydrocarbon Systems. Volumetric and Phase Behavior of the Methane-n-Butane System at Higher Pressures. *Ind. Eng. Chem. Ind. Ed.* **1947**, *39*, 206–209.

Reamer, H. H.; Sage, B. H.; Lacey, W. N. Phase Equilibria in Hydrocarbon Systems. Volumetric and Phase Behavior of the Methane-Propane System. *Ind. Eng. Chem. Ind. Ed.* **1950**, *42*, 534–539.

Rijkers, M. P. W. M.; Malais, M.; Peters, C. J.; de Swann Arons J. Measurement on the Phase Behavior of Binary Hydrocarbon Mixtures for Modeling the Condensation Behavior of Natural Gas. Part I. The System Methane + Decane. *Fluid Phase Equilib.* **1992a**, *71*, 143–168.

Rijkers, M. P. W. M.; Maduro, V. B.; Peters, C. J.; de Swann Arons J. Measurement on the Phase Behavior of Binary Hydrocarbon Mixtures for Modeling the Condensation Behavior of Natural Gas. Part II. The System Methane + Dodecane. *Fluid Phase Equilib.* **1992b**, *72*, 309–324.

Rijkers, M. P. W. M.; Peters, C. J.; de Swann Arons J. Measurement on the Phase Behavior of Binary Hydrocarbon Mixtures for Modeling the Condensation Behavior of Natural Gas. Part III. The System Methane + Hexadecane. *Fluid Phase Equilib.* **1993**, *85*, 335–345.

Sage, B. H.; Lacey, W. N.; Schaafsma, J. G. Phase Equilibria in Hydrocarbon Systems. II. Methane-Propane System. *Ind. Eng. Chem. Ind. Ed.* **1934**, *26*, 214–217.

Sage, B. H.; Lacey, W. N.; Schaafsma, J. G. Phase Equilibria in Hydrocarbon Systems. The Methane-Ethane System in the Gaseous Region. *Ind. Eng. Chem. Ind. Ed.* **1939**, *31*, 1497–1509.

Sage, B. H.; Budenholtzer, R. A.; Lacey, W. N. Phase Equilibria in Hydrocarbon Systems. Methane-n-Butane System in the Gaseous and Liquid Region. *Ind. Eng. Chem. Ind. Ed.* **1940a**, *32*, 1262–1277.

Sage, B. H.; Lavender, H. M..; Lacey, W. N. Phase Equilibria in Hydrocarbon Systems. Methane-Decane System. *Ind. Eng. Chem. Ind. Ed.* **1940b**, *32*, 743–747.

Sage, B. H.; Reamer, H. H.; Olds, R. H.; Lacey, W. N. Phase Equilibria in Hydrocarbon Systems. Volumetric and Phase Behavior of Methane-Pentane System. *Ind. Eng. Chem. Ind. Ed.* **1942**, *34*, 1108–1117.

Shim, J. J.; Johnston, K. P. Phase Equilibria, Partial Molar Enthalpies, and Partial Molar Volumes Determined by Supercritical Fluid Chromatography. *J. Phys. Chem.* **1991**, *95*, 353–360.

Smith, R. D.; Udseth, H. R.; Wright, B. W.; Yonker, C. R. Solubilities in Supercritical Fluids: The Application of Chromatographic Measurement Methods. *Sep. Sci. Technol.* **1987**, *22*, 1065–1086.

Suleiman, D.; Gurdial, G. S.; Eckert, C. A. An Appparatus for Phase Equilibria of Heavy Paraffins in Supercritical Fluids. *AIChE J.* **1993**, *39*, 1257–1260.

van Wasen, U.; Swaid, I.; Schneider, G. M. Physicochemical Principles and Applications of Supercritical Fluid Chromatography *Angew. Chem., Int. Ed. Engl.* **1980**, *19*, 575–587.

Yonker, C. R.; Wright, R. W.; Frye, S. L.; Smith, R. D. Mechanism of Solute Retention in Supercritical Fluid Chromatography. *ACS Symp. Ser.* **1987**, *329*, 172–188.

Younglove, B. A.; Ely, J. F. Thermophysical Properties of Fluids. II. Methane, Ethane, Propane, Isobutane, and Normal Butane. *J. Phys. Chem. Ref. Data* **1987**, *16*, 577–798.

Received for review July 11, 1994. Accepted October 24, 1994.[⊗] We gratefully acknowledge the financial support from the GRI (Gas Research Institute) and the GPA (Gas Processors Association).

JE940138V

[⊗] Abstract published in *Advance ACS Abstracts,* December 1, 1994.